

# A technique for measuring solar differential rotation

Peter Meadows

The Sun exhibits differential rotation, with its rotation rate or period varying with heliographic latitude. This short paper demonstrates a method for using full-disc white-light solar images to measure the Sun's rotation rate at different latitudes. Using images from the *Solar Dynamics Observatory*, suitable sunspots are selected. The central meridian distance of these sunspots is calculated, and the synodic rotation rates are determined. The paper also explains how to convert synodic to sidereal rotation rates and derive parameters for a differential rotation model. Results are compared with other studies, showing consistency despite the relatively small number of measurements.

## Introduction

As the Sun is a gaseous rotating body consisting primarily of hydrogen and helium, it is to be expected that its rotation rate, in degrees of longitude per day ( $^{\circ}/\text{day}$ ), or rotation period, in days, will vary depending on the heliographic latitude above or below the equator. Full-disc white-light solar images can be used to show that the Sun indeed exhibits differential rotation, measure the rotation rate at different latitudes, and derive the parameters for a differential rotation model.

Many of the full-disc solar images contributed to the BAA Solar Section or available from other sources are suitable for deriving rotation rates. The main requirement is that the images have accurate orientation. This can be either equatorial (usually celestial north at the image top and east to the image left), with the solar rotation axis in the vertical direction (as for solar satellite images), or altazimuth.

Provided several images are available of the same sunspot as it progresses across the solar disc, then the author's *HelioViewer* software tool can be used to measure the latitude and longitude of the sunspot and then calculate the central-meridian distance ( $D_{\text{CM}}$ ; the longitude difference between the sunspot and the central meridian of the Sun).<sup>1</sup> As will be shown, the CMD distances can be easily calculated using a spreadsheet such as Microsoft *Excel* and then used to calculate the rotation rate of a particular sunspot. By measuring the rotation rate of sunspots at different latitudes, the parameters of the differential rotation model can be deduced, again using a spreadsheet.

The following section describes the selection of suitable sunspots. Here, solar images from the *Solar Dynamics Observatory* (SDO) satellite and the Helioseismic & Magnetic Imager (HMI) Continuum instrument have been used,<sup>2</sup> but the same steps can be

used for other full-disc solar images. Then, the steps to measure the sunspot position and calculate the CMD are described, followed by the calculation of the solar rotation rate for a particular sunspot. This rotation rate is the synodic rate (i.e., as measured from Earth). So, before comparing the rotation rate of many sunspots, using imagery taken at different times of the year, a conversion to sidereal rotation rate needs to be performed.

It is then shown how the parameters to a differential rotation model can be easily calculated, again using a spreadsheet. Next, the derived rotation model is compared with a selection of previous studies. A subset of measurements is described that would be suitable for a student project into the nature of solar rotation. Conclusions are then presented.

Note that the purpose of this paper is to demonstrate the differential nature of the Sun's rotation using a relatively small number of sunspots and measurements, rather than to present a comprehensive study of solar rotation.

## Sunspot selection

The choice of sunspots to measure the rotation rate is important. Within most groups, sunspots have their own proper motion with respect to the photosphere and hence with respect to the general rotation of the Sun, which we want to measure. Also, many groups have a rapid increase in size and complexity followed by a slower decrease in size before disappearing – again, sunspots within such groups are not ideal due to their proper motion.

It is suggested here that the most suitable sunspots are those that change very little during their passage across the solar disc. These are single, isolated, unipolar

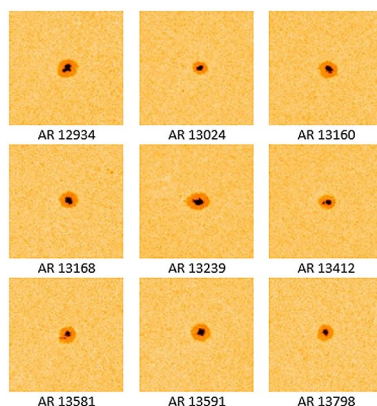


Figure 1. Examples of selected H-type sunspots.

**Table 1. Selected sunspot groups**

NOAA active region no.	Date on central meridian	Day of year on central meridian	Mean lat. (°)	Mean long. (°)	Synodic rotation rate (°/day)	$\Psi$ (°/day)	Sidereal rotation rate (°/day)
12785	2020 Nov 28	333	-22	2	13.30	1.01	14.31
12818	2021 Apr 26	116	-16	204	13.23	0.97	14.21
12886	2021 Oct 23	296	-19	333	13.11	1.00	14.10
12927	2022 Jan 15	15	-20	317	13.17	1.02	14.19
<b>12934</b>	<b>2022 Jan 26</b>	<b>26</b>	<b>-25</b>	<b>170</b>	<b>12.95</b>	<b>1.02</b>	<b>13.97</b>
<b>13024</b>	<b>2022 May 31</b>	<b>151</b>	<b>-34</b>	<b>317</b>	<b>12.47</b>	<b>0.96</b>	<b>13.43</b>
13071	2022 Aug 08	220	-18	126	13.29	0.96	14.25
<b>13160</b>	<b>2022 Dec 12</b>	<b>346</b>	<b>23</b>	<b>258</b>	<b>13.02</b>	<b>1.02</b>	<b>14.04</b>
<b>13168</b>	<b>2022 Dec 20</b>	<b>354</b>	<b>-16</b>	<b>160</b>	<b>13.25</b>	<b>1.02</b>	<b>14.27</b>
13201	2023 Jan 29	29	24	351	13.13	1.02	14.15
<b>13239</b>	<b>2023 Mar 06</b>	<b>66</b>	<b>33</b>	<b>237</b>	<b>12.61</b>	<b>1.00</b>	<b>13.62</b>
13241	2023 Mar 07	66	28	223	12.61	1.00	13.61
13264	2023 Mar 30	89	15	280	13.07	0.99	14.05
13326	2023 Jun 08	159	25	69	13.12	0.96	14.08
13362	2023 Jul 10	191	-8	9	13.33	0.95	14.28
<b>13412</b>	<b>2023 Aug 24</b>	<b>236</b>	<b>31</b>	<b>134</b>	<b>12.75</b>	<b>0.97</b>	<b>13.71</b>
13501	2023 Nov 29	333	-9	297	13.44	1.01	14.45
<b>13581</b>	<b>2024 Feb 14</b>	<b>45</b>	<b>-21</b>	<b>1</b>	<b>13.05</b>	<b>1.01</b>	<b>14.06</b>
<b>13591</b>	<b>2024 Feb 29</b>	<b>60</b>	<b>-36</b>	<b>160</b>	<b>12.55</b>	<b>1.00</b>	<b>13.56</b>
13690	2024 May 29	150	16	53	13.48	0.96	14.44
13756	2024 Jul 22	204	-17	67	13.32	0.96	14.28
<b>13798</b>	<b>2024 Aug 25</b>	<b>238</b>	<b>6</b>	<b>330</b>	<b>13.47</b>	<b>0.97</b>	<b>14.43</b>
13937	2024 Dec 28	363	-12	116	13.25	1.02	14.27
13989	2025 Feb 15	46	19	204	12.92	1.01	13.93

Note: The sunspots shown in bold make up a subset suitable for measurement in a student project. See text for details.

penumbral sunspots of type H,<sup>3</sup> which change little for many days at a time. Preferably, they should not develop any surrounding pores and should not start to decay.

SDO/HMI images were visually examined from the start of 2020 (i.e., from the start of Cycle 25) to the end of 2025 February for the identification of isolated H-type sunspots. Table 1 shows 24 sunspots that have been chosen as being suitable for determining the solar rotation rate. They vary in heliographic latitude between 33°N and 36°S, and there are slightly more of them in the southern hemisphere (14 compared to 10) due to dominance of southern-hemisphere activity during the first half of Cycle 25. The average area of the 24 sunspots is 110 millionths of the Sun's visible hemisphere. Figure 1 shows nine example H-type sunspots.

Note that Table 1 gives the US Air Force (USAF) and National Oceanic and Atmospheric Administration (NOAA) Active Region number,<sup>4</sup> and the date and day of year (DoY) when the sunspot was close to the central meridian, together with the measured sunspot location and derived rotation rate.

## Sunspot location measurement

The heliographic latitude and longitude can be measured using *HelioViewer*, as shown in Figure 2 with an example SDO/HMI image containing Active Region (AR) 13239 from 2023 March 5. Once the image is loaded into *HelioViewer*, the date, time and

orientation are automatically set correctly (see Appendix A), then a left click on the middle of the sunspot enables its latitude and longitude to be calculated and displayed on the left-hand side of the *HelioViewer* window. *HelioViewer* also shows the longitude of the central meridian ( $L_0$ ). The CMD is calculated by:

$$D_{\text{CM}} = L - L_0 \quad (1)$$

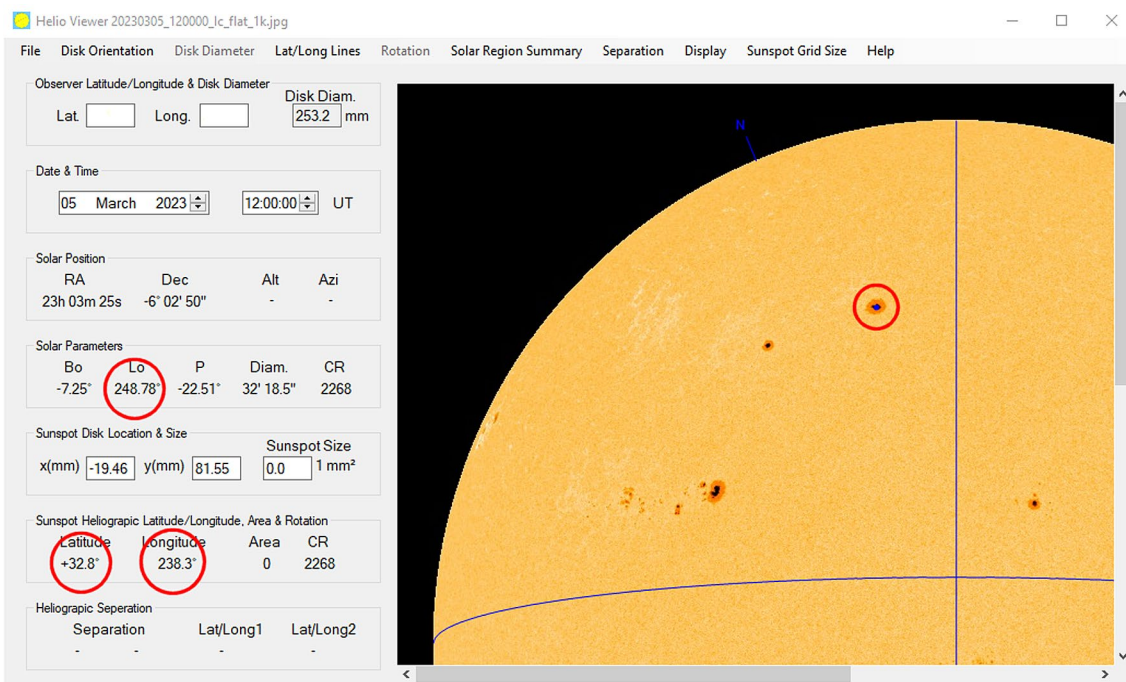
where  $L$  is longitude. Note that CMD has a range of between  $-90^\circ$  (east) and  $+90^\circ$  (west), and if the calculated CMD is outside this range, then  $360^\circ$  needs to be added or subtracted.

Table 2 gives example positions and CMD measurements for AR 13239 from 2023 March, using SDO/HMI images spaced 12 hours apart. There are no data points for March 6 (DoY 66), as this sunspot became a type-C group before reverting back to type H.

To avoid any projection effects when sunspots are near to the limb, measurements were only made where the CMD is between  $-60$  and  $+60^\circ$ . This corresponds to between five days before and five days after the sunspot was closest to the central meridian.

## Calculation of rotation rate

The rotation rate of an individual sunspot can be easily calculated by plotting the DoY against CMD.<sup>5</sup> An example plot using *Excel*,<sup>6</sup> for the sunspot AR 13239 data in Table 2, is shown in



**Figure 2.** *HelioViewer* with SDO/HMI image from 2023 March 5, showing the location of AR 13239 (blue dot within right-hand red circle) together with the sunspot heliographic latitude and longitude, and the longitude of the central meridian,  $L_0$  (left-hand red circles).

Figure 3: there is a good linear relationship between DoY and CMD. Figure 3 also includes a linear-fit dashed line, the line equation, and goodness-of-fit parameter  $R^2$ .<sup>7</sup> The slope of the line is the synodic rotation rate for the sunspot in  $^\circ/\text{day}$ . The same approach is then repeated for each sunspot.

Table 1 gives the synodic rotation rate for each of the 24 sunspots used in this paper. Note that for all sunspots,  $R^2$  is equal to 1.0 (to four decimal places).

### Conversion from synodic to sidereal rotation rate

Figure 4 shows the difference between the rotation of the Sun as seen from Earth (the synodic rotation), and relative to the fixed stars (the sidereal rotation – the fixed stars are located to the extreme left of the Figure). At date  $t_1$ , a sunspot on the Sun’s central



**Figure 3.** CMD for AR 13239 between 2023 Mar 2 and Mar 11. A linear fit is shown as a dashed line. The slope of the linear fit equation (top right) in *Excel* gives a synodic rotation rate of 12.61 $^\circ/\text{day}$ .

meridian is shown by the blue dot. One solar rotation later, Earth’s position has rotated on its orbit around the Sun to the location at date  $t_2$ . The same sunspot, again on the central meridian, is shown by the red dot. During the period between dates  $t_1$  and  $t_2$ , the Sun has rotated, with respect to the fixed stars, by  $360^\circ$  plus the angle  $\theta$ . Thus, the synodic rotation period is longer than the sidereal rotation period. Over the period of a year,  $\theta$  is  $360^\circ$ .

If Earth’s orbit were circular and the Sun’s rotation axis were orthogonal to it, the daily difference between the synodic and sidereal rotation rates, denoted by  $\psi$ , would simply be  $360^\circ$  per 365.25 days or  $0.9856^\circ/\text{day}$ .

Considering only the variation in Earth’s distance from the Sun during the year (i.e., ignoring the Sun’s inclination to the ecliptic), a more accurate value for  $\psi$  can be calculated.<sup>8,9</sup> This has an error of less than  $0.01^\circ$ , which is adequate for this paper. The yearly variation in  $\psi$  is shown in Figure 5, and the algorithm to calculate  $\psi$  is given in Appendix B. The conversion from synodic rate,  $\omega_{\text{syn}}$ , to sidereal rate,  $\omega_{\text{sid}}$ , is given by:

$$\omega_{\text{sid}} = \omega_{\text{syn}} + \psi \tag{2}$$

Also included in Table 1 is  $\psi$  and the sidereal rates for the selected sunspots, based on the date when the sunspot is closest to the central meridian. Figure 6 shows the variation of the sidereal rotation rate with latitude for the 24 selected sunspots.

### Fitting of the differential rotation model

The equation to describe the sidereal differential rotation rate is given by:

$$\omega_{\text{sid}} = A + B \sin^2(\varphi) + C \sin^4(\varphi) \tag{3}$$

Model parameter  $A$  is the rotation rate at the equator, while parameters  $B$  and  $C$  give the rotation dependence on heliographic latitude,  $\varphi$ . The parameter  $C$  is important for high solar latitudes and so can be ignored for sunspots.<sup>9</sup> Thus,  $C$  is set to zero.

The standard equation of a straight line is  $y = mx + c$  where the data coordinates are  $(x, y)$ , the line slope is  $m$  and the intercept on the  $y$ -axis is  $c$ . Equation 3 can be rewritten as:

$$\omega_{\text{sid}} = B \sin^2(\varphi) + A \tag{4}$$

Therefore, plotting  $\sin^2(\varphi)$  against  $\omega_{\text{sid}}$  will give a linear fit where the slope and intercept give values for  $B$  and  $A$ , respectively.

Figure 7 shows a plot of  $\sin^2(\varphi)$  against  $\omega_{\text{sid}}$  for the selected sunspots, where the upper right of the plot gives  $A = 14.46$  °/day and  $B = -2.83$  °/day. The differential rotation curve using these parameter values is also shown in Figure 6. The sidereal equatorial rotation period can be calculated from  $360^\circ/A = 24.90$  days, while Equation 4 can be used to calculate, for example, the sidereal rotation period at a latitude of  $\pm 30^\circ$  as 26.18 days.

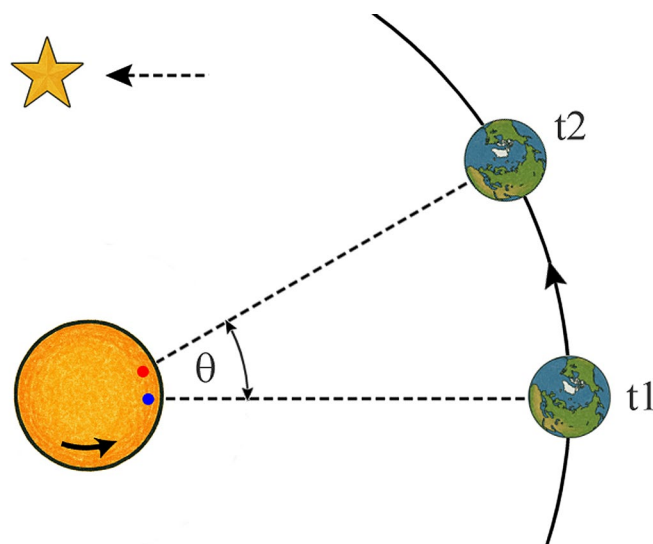


Figure 4. Illustration of the difference between synodic and sidereal rotation of the Sun. See text for details.

## Discussion

If it is assumed that the differential rotation fit shown in Figure 6 is an exact representation of the solar differential rotation, then all 24 sunspots would lie precisely on the model curve. However, this is not the case. The most likely explanation is that these sunspots exhibit a proper motion in longitude.

Table 3 presents four sets of differential rotation rate parameters from previous studies, alongside the results from this study. The findings here are comparable to those of the other studies, despite the relatively small number of rotation rate measurements taken.

Stix (2002) and Brajša & Hanslmeier (2024) note that the equatorial rotation rate (parameter  $A$ ) for recurrent sunspots, which include long-lived H-type sunspots, is shorter than that derived from studies using all types of sunspot groups.<sup>9,12</sup> It is evident in Table 3 that there is a distinction between studies focusing on isolated or recurrent sunspots and those analysing a large number of sunspot groups of all types. The difference is attributed to a drag in the photosphere affecting recurrent sunspots.

The equatorial rotation rate derived in this study falls between the values reported for isolated/recurrent sunspots and those for all sunspot groups. None of the selected H-type groups in this study were observed for more than one rotation and therefore they cannot be classified as recurrent. A larger sample of sunspot groups and a longer time period would enable determination of more definitive values for the equatorial rotation model parameters.

## Measurement subset for students

The results presented here are based on 24 sunspots and SDO images acquired at 12-hour intervals, which requires 300 individual heliographic latitude and longitude measurements.<sup>13</sup> A student, with limited time, but still with the aim of demonstrating the differential rotation of the Sun, can use a subset of sunspots and

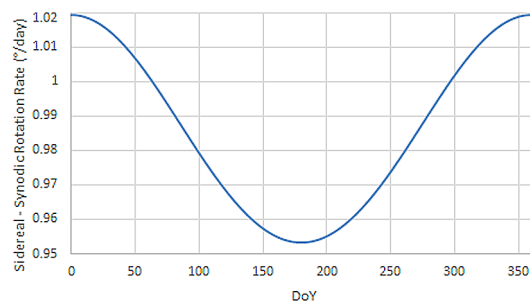


Figure 5. Difference between sidereal and synodic solar-rotation rates during the year.

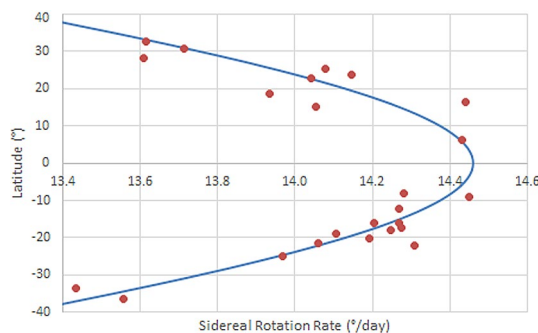


Figure 6. Relationship between sidereal rotation rate and heliographic latitude for the selected sunspot groups in Table 1. The curve is the best fit to the differential rotation model.

measurements. By selecting the nine sunspots shown in bold in Table 1 and those in Figure 1, together with using images approximately two days apart, then the number of measurements using *HelioViewer* could be reduced to a more manageable 50. The nine sunspots have been selected to cover the full range of latitudes and to give similar values for the differential rotation model parameters  $A$  and  $B$  as for the full set of measurements (see Table 3).

**Table 2. Position & central-meridian distance measurements for AR 13239**

Date	Time (UT)	DoY	$L_0$ (°)	Lat. (°)	Long. (°)	CMD (°)
2023 Mar 2	00:00	61.0	295.0	32.4	239.6	-55.4
2023 Mar 2	12:00	61.5	288.4	32.3	239.5	-48.9
2023 Mar 3	00:00	62.0	281.8	32.3	239.3	-42.5
2023 Mar 3	12:00	62.5	275.2	32.4	239.0	-36.2
2023 Mar 4	00:00	63.0	268.6	32.5	238.9	-29.7
2023 Mar 4	12:00	63.5	262.0	32.6	238.7	-23.3
2023 Mar 5	00:00	64.0	255.4	32.7	238.5	-16.9
2023 Mar 5	12:00	64.5	248.8	32.8	238.3	-10.5
2023 Mar 7	00:00	66.0	229.1	33.1	237.4	8.3
2023 Mar 7	12:00	66.5	222.5	33.1	237.0	14.5
2023 Mar 8	00:00	67.0	215.9	33.1	236.8	20.9
2023 Mar 8	12:00	67.5	209.3	33.1	236.4	27.1
2023 Mar 9	00:00	68.0	202.7	33.0	236.1	33.4
2023 Mar 9	12:00	68.5	196.1	32.9	235.7	39.6
2023 Mar 10	00:00	69.0	189.6	32.8	235.3	45.7
2023 Mar 10	12:00	69.5	183.0	32.7	234.9	51.9
2023 Mar 11	00:00	70.0	176.4	32.6	234.7	58.3

It is envisaged that a template spreadsheet could be created where students would only need to enter the sunspot position information and the longitude of the central meridian. In addition, the various calculations and plots could already be included in the spreadsheet to reduce the time required by the student.

## Conclusions

This study has demonstrated the differential rotation of the Sun using a modest yet representative set of 24 isolated H-type sunspots observed across a range of heliographic latitudes. By using full-disc SDO/HMI white-light images, alongside the *HelioViewer* tool and spreadsheet analysis, it was possible to calculate accurate synodic rotation rates for each sunspot. These were then converted to sidereal rates, allowing for the derivation of differential rotation model parameters.

The resulting fit to a solar differential rotation model, using parameters  $A = 14.46$  °/day and  $B = -2.83$  °/day, is in good

agreement with values reported in previous studies. Although the sunspots do not lie exactly on the fitted curve – likely due to their inherent proper motion – the overall consistency supports the validity of this short study. Importantly, the equatorial rotation period derived here (24.90 days) lies between values obtained for recurrent sunspots and those obtained using all sunspot group types.

While the sample size and time period are limited, this paper has shown that the differential nature of the Sun's rotation can be effectively demonstrated using a relatively small number of carefully selected sunspots. This makes the approach particularly suitable for educational purposes, where time constraints may apply. A reduced dataset of nine sunspots has been proposed for student investigations, along with the suggestion of a pre-configured spreadsheet to streamline the analysis.

Further work involving a larger dataset over a longer time span would allow for more precise determination of the Sun's rotation profile, particularly at higher latitudes. However, even with limited data, the methodology outlined here offers a robust and accessible means of quantifying solar rotation.

**Table 3. White-light differential sidereal solar-rotation rates**

Source	$A$ (°/day)	$B$ (°/day)	$C$ (°/day)	Comments
Maunder <sup>10</sup>	14.37	-2.60	0.00	Based on small, isolated sunspot from 1888–1893
Newton & Nunn <sup>11</sup>	14.38	-2.96	0.00	Based on single recurrent sunspots from 1934–1944
Stix <sup>12</sup>	$14.54 \pm 0.02$	$-2.86 \pm 0.02$	0.00	Average of Greenwich (1874–1976) sunspot groups & Mt Wilson (1921–1982) individual sunspots
Brajša & Hanslmeier <sup>14</sup>	$14.50 \pm 0.05$	$-2.67 \pm 0.20$	0.00	Average of 11 datasets from Greenwich, <i>Debrecen Photoheliographic Data</i> catalogue and Kanzelhöhe for sunspot groups and individual sunspots
This paper	14.46	-2.83	0.00	Based on 24 isolated individual sunspots (Table 1)
This paper	14.47	-2.89	0.00	Based on nine isolated individual sunspots (bold entries in Table 1)

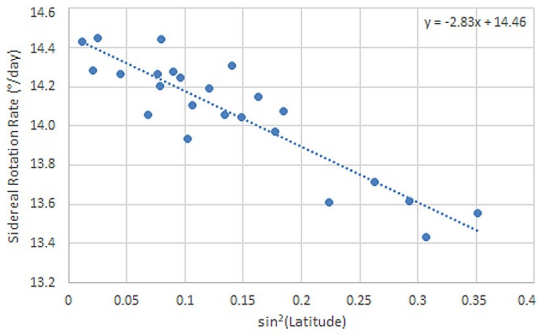


**Figure 7.** Relationship between  $\sin^2(\text{latitude})$  and sidereal rotation rate for the selected sunspot groups in Table 1. The dashed line is a linear fit whose equation (top right) gives the  $A$  (14.46 °/day) and  $B$  (−2.83 °/day) parameters for the differential rotation model.

## Acknowledgements

Two referees are thanked for their constructive comments that have improved this paper. The SDO HMI Continuum images are courtesy of NASA/SDO and the HMI science team.

**Address:** 11 Pavitt Meadow, Galleywood, Chelmsford, Essex CM2 8RQ [peter@petermeadows.com]

## Appendix A

### Using HelioViewer

Prior to using *HelioViewer* for the sunspot position measurement, the following steps are needed:

- **Set the correct orientation.** The equatorial orientation, for example, is set by using menu Disk Orientation > Equatorial. The other options are AltAzimuth or Rotation Axis (mainly for satellite solar images). In addition, a change of east/west position can be made using menu Disk Orientation > Mirror. Usually, images have east towards the left (and north towards the top). Note that for SDO/HMI flattened images, the orientation is automatically set (based on the filename containing the string ‘\_lc\_flat\_1k’).
- **Set the image size.** If the input image is large – at more, say, than approximately  $1,000 \times 1,000$  pixels – it is suggested that the image size is reduced using, for example, menu Display > Image Size > Reduce / 2, to reduce the size by a factor of 2. This needs to be set before opening the image (menu File > Open Image...).
- **Set the latitude and longitude precision.** It is suggested that this is set to  $0.1^\circ$  using menu Display > Lat Long >  $0.1^\circ$ .

## Appendix B

### Conversion from synodic to sidereal rotation rate

An approximate set of equations for the conversion from the synodic to sidereal rotation rate for a particular sunspot is given by Graf (1974),<sup>8</sup> and corrected by Brajša & Hanslmeier (2024).<sup>9</sup> This approach only takes into account the variation in Earth’s distance from the Sun during the year (i.e., ignoring the Sun’s inclination to the ecliptic) to calculate the difference between the synodic and sidereal rotation rates ( $\psi$ ):

$$\psi = \psi_0 / D^2$$

where  $\psi_0$  has a value of 3547.717 arcsec or  $0.9855^\circ$ , and  $D$  is the Earth–Sun distance in astronomical units.

The distance  $D$  is given by the equation:

$$D = 1.0 - e \cos(T + e \sin(T))$$

where  $e$  is the eccentricity of Earth’s orbit ( $= 0.01675$ ) and  $T$  is the fraction of the year from the date of perihelion and is equal to  $(2\pi / 365.25) \times (t_{DoY} - t_{PH})$ .  $t_{DoY}$  is the number of days after January 0 and  $t_{PH}$  is the time in days of the mean perihelion: a value of 3.5 has been assumed.

If using *Excel*, the following steps are required, where the value of  $t_{DoY}$  for when the sunspot is closest to the central meridian (see Table 1) is input into cell A1:

- $T$  is calculated in cell B1 using the expression ‘ $(2*PI()/360)*(A1-3.5)$ ’
- $D$  is calculated in cell C1 using the expression ‘ $=1-0.01675*COS(B1+0.01675*SIN(B1))$ ’
- $\psi$  is calculated in cell D1 using the expression ‘ $=0.9855/(C1*C1)$ ’

Note that  $\psi$  is in °/day and as  $T$  is already in radians, no conversion from degrees to radians for the *Excel* sin and cos functions is required for the calculation of  $D$ .

## References & notes

- 1 Meadows P., *HelioViewer* v.2.3 [software]: <https://www.petermeadows.com/html/software.html> (accessed 2026 April 25). Note the comments at the top of the page and then scroll to the ‘HelioViewer’ section, at the bottom of which the link to download the zip file can be found.
- 2 SDO HMI images can be obtained from the Joint Science Operations Center website: <http://jsoc.stanford.edu/HMI/hmiimage.html> (accessed 2026 April 25). Select the date and time, then choose ‘Flattened Intensity’ for the data type and ‘1024’ for the resolution before pressing the ‘Display HMI Image’ button. Alternatively, they can be obtained from <https://jsoc1.stanford.edu/data/hmi/images/>, where after selecting the year, month and day, a filename of the form `yyyymmdd_hhmmss_lc_flat_1k.jpg` can be downloaded. These images have a typical cadence of 15 minutes.
- 3 McIntosh P. S., ‘The classification of sunspot groups’, *Solar Physics*, **125**, 251–267 (1990) doi.org/10.1007/BF00158405
- 4 Note that the USAF/NOAA Active Region (AR) number can be given either as a five- or four-digit number, the latter being a shortened version of the former. The numbering began in 1972 January, with the number of ARs passing 10,000 in 2002 June and so currently the five-digit version has a leading 1. See: <https://hesperia.gsfc.nasa.gov/rhessi3/public-outreach/the-solar-faq/index.html> (accessed 2026 April 25).
- 5 The Day of Year can be calculated in Microsoft *Excel* software from the date in, say, cell B2 by using the expression ‘ $B2 - DATE(YEAR(B2),1,1)+1$ ’, where cell B2 is in date format.
- 6 Microsoft Corporation, *Microsoft Excel* [software]: <https://office.microsoft.com/excel> [accessed 2026 May 5]
- 7 In the *Excel* plot, the dashed line is created by right-clicking on any data point, selecting ‘Add Trendline...’, selecting the ‘Linear’ option and then ticking the ‘Display Equation’ and ‘Display R-squared’ boxes to show the equation and goodness of fit parameter  $R^2$  on the plot.
- 8 Graf W., ‘Yearly variation on the synodic rotation period of the Sun’, *Solar Physics*, **37**, 257–260 (1974) doi.org/10.1007/BF00157862
- 9 Brajša R. & Hanslmeier A., *Solar Rotation*, Springer, Berlin Heidelberg, 2024 doi.org/10.1007/978-981-97-6879-0
- 10 Abetti G., *The Sun*, Faber & Faber, London, 1959, p. 89
- 11 H. W. Newton & M. L. Nunn, ‘The Sun’s rotation derived from sunspots 1934–1944 and additional results’, *Mon. Not. R. Astron. Soc.*, **111**(4), 413–421 (1951) doi.org/10.1093/mnras/111.4.413
- 12 Stix M., *The Sun: An Introduction*, 2nd ed., Springer, Berlin, 2002, p. 290 doi:10.1007/978-3-642-56042-2
- 13 The measurements presented in this paper have been deduced using the author’s PYTHON script to automatically extract sunspots from an SDO/HMI image, identify individual sunspot groups and calculate their position, area and McIntosh classification. For the latest SDO images, see <https://petermeadows.com/SDOSunspotGroups/> (accessed 2026 April 25).
- 14 Brajša R. & Hanslmeier A., *op. cit.*, Figure 6.8

Received 2025 March 14; accepted 2025 June 4